International Journal of Neural Systems, Vol. 25, No. 3 (2015) 1550011 (12 pages)

DOI: 10.1142/S0129065715500112

World Scientific
www.worldscientific.com

A P300 Brain–Computer Interface Based on a Modification of the Mismatch Negativity Paradigm

Jing Jin*
Key Laboratory of Advanced Control and Optimization for Chemical Processes
Ministry of Education, East China University of Science and Technology
Shanghai 200237, China
jinjingat@gmail.com

Eric W Sellers
Brain-Computer Interface Laboratory
Department of Psychology
East Tennessee State University
37614 Johnson City, TN, USA
SELLERS@mail.etsu.edu

Sijie Zhou†, Yu Zhang‡ and Xingyu Wang§
Key Laboratory of Advanced Control and Optimization for Chemical Processes
Ministry of Education, East China University of Science and Technology
Shanghai 200237, China
†*zhou.sijie@foxmail.com*
‡*yuzhang@ecust.edu.cn*
§*xywang@ecust.edu.cn*

Andrzej Cichocki
Laboratory for Advanced Brain Signal Processing
Brain Science Institute, RIKEN, Wako-shi 351-0198, Japan
Systems Research Institute of Polish Academy of Science, Warsaw, Poland
cia@brain.riken.jp

Accepted 3 February 2015
Published Online 25 March 2015

The P300-based brain–computer interface (BCI) is an extension of the oddball paradigm, and can facilitate communication for people with severe neuromuscular disorders. It has been shown that, in addition to the P300, other event-related potential (ERP) components have been shown to contribute to successful operation of the P300 BCI. Incorporating these components into the classification algorithm can improve the classification accuracy and information transfer rate (ITR). In this paper, a single character presentation paradigm was compared to a presentation paradigm that is based on the visual mismatch negativity. The mismatch negativity paradigm showed significantly higher classification accuracy and ITRs than a single character presentation paradigm. In addition, the mismatch paradigm elicited larger N200 and N400 components than the single character paradigm. The components elicited by the presentation method were consistent with what would be expected from a mismatch paradigm and a typical P300 was also observed. The results show that increasing the signal-to-noise ratio by increasing the amplitude of ERP components can significantly improve BCI speed and accuracy. The mismatch presentation paradigm may be considered a viable option to the traditional P300 BCI paradigm.

Keywords: Brain computer interface; event-related potentials; mismatch negativity.

*Corresponding author.

1. Introduction

Brain–computer interface (BCI) technology provides people with a means of communication, or a method to send commands to external devices in real time. Noninvasive BCIs typically rely on the scalp-recorded electroencephalogram (EEG).[1–16] The P300-based BCI was introduced by Farewell and Donchin.[17] They showed that the P300 event-related potential (ERP) could be used to successfully select a letter when the subject focused on a target letter and counted how many times the letter flashed. However, it is necessary to average several ERPs for the P300 BCI to obtain high accuracy. The major deleterious side effect of averaging is that it increases the amount of time needed to make a character selection, thereby decreasing information transfer rate (ITR).[18–20]

Many studies have examined ways to improve P300 BCI performance. Several studies have focused on classifier optimization.[21–26] Lenhardt *et al.*[27] and Jin *et al.*[28] improved classification accuracy and ITR using strategies that dynamically adapted the number of trials used to make character selections. Zhang *et al.*,[31] presented spatiotemporal discriminant analysis to decrease the amount of time needed for offline training. In addition, Lu *et al.*,[29] and Jin *et al.*[30] presented generic model strategies that obviated the need for offline training. In addition to classification methods, several studies have focused on reducing the overlap of target epochs and decreasing interference created by items adjacent to the target.[27,32–34] Target-to-target interval and inter-stimulus interval (ISI) have also been used to optimize the stimulus sequence.[32,35–38]

In addition to developing new classification methods, novel stimulus presentation paradigms have been proposed. In general, these paradigms have been developed to exploit ERP components in addition to the P300, and to enhance the difference between attended and ignored events. The majority of spatiotemporal features selected by classification algorithms occur at locations and latencies consistent with the P300.[39] However, stimulus parameters can be manipulated so that additional ERP components will be elicited, and contribute to the classification algorithm. For example, Hong *et al.*[40] replaced flashes with motion stimuli that could elicit N200s, which could provide performance that was superior to a conventional P300 BCI paradigm. Jin *et al.*[41] combined motion and flash stimuli, which increased the amplitude of the N200 and P300 components and resulted in higher accuracy and IRT.

The mismatch negativity (MMN) was first demonstrated by Näätänen *et al.*[42] using auditory stimuli. In the experiment, a rare deviant (D) sound

(a) (b) (c)

Fig. 1. (Color online) The display presented to the subjects. (a) The 3×4 matrix used in the study with 12 commands (flashes). (b) The green rectangle indicated the target character for the current trial. (c) Top: example of the SC-pattern. Bottom: an example of the MSC-pattern. Feedback is presented at the top of the screen.

was interspersed among a series of frequent standard (S) sounds (e.g. S/S/S/S/S/D/S/S/S/D/S/S/S/S/S, "/" denotes the ISI). The MMN paradigm has been used as a two-choice auditory-based BCI.[43,44] The visual stimulus modality also elicits a MMN (i.e. the vMMN).[45–51] Consistent with the auditory MMN, the vMMN elicits an N200 and it also elicits a large P300.[46,47] Until now, the vMMN has not been used in the context of a BCI task. In this paper, a vMMN presentation paradigm is compared to a single character paradigm. The typical visual P300 BCI paradigm presents the subject with a matrix of items and the rows and columns of the matrix flash at random.[17] Instead of flashing groups of rows and columns, the single character pattern (SC-pattern) flashes a single matrix item.[52] In this study, we compare an SC-pattern to a mismatch single character pattern (MSC-pattern; see Fig. 1 for example stimuli). The MSC-pattern was designed to evoke a larger MMN (i.e. N200) as compared to the SC-pattern. Our hypotheses are that the MSC-pattern will increase N200 and P300 amplitudes, and that the MSC-pattern will increase P300 BCI performance.

2. Method and Materials

2.1. *Subjects and stimuli*

Ten healthy subjects (eight male and two female, aged 21–25, mean 23.1 ± 1.5) were paid to participate in the study. All subjects' native language was Mandarin Chinese, and all subjects were familiar with the Western characters used in the display. Three subjects had used a BCI before this study. During data acquisition, subjects were asked to relax and avoid unnecessary movement.

Subjects were seated about 85 cm in front of a monitor that was 30 cm long and 48 cm wide. The display presented to the subjects is shown in Fig. 1. Twelve items were presented in a 3×4 arrangement. The subjects' task was to focus attention to the desired character in the matrix and count the number of times the letter 'D' flashed directly above the character. Before the experiment, the task was explained and demonstrated to the subjects. The experiment was started when the subject was able to properly perform the task and had no additional questions.

In the SC-pattern, the letter D (i.e. deviant) was presented at random above each of the 12 items (Fig. 1(c), top panel). The MSC-pattern was the same as the SC-pattern with one exception. When the D was flashed above one of the items, a gray S (standard) flashed above the other 11 items (Fig. 1(c), bottom panel), thereby producing a "visual mismatch". In each trial, the ISI was 100 ms and the stimulus onset asynchrony (SOA) was 300 ms. Each trial consisted of 12 flashes. That is, the letter D (deviant) was presented above all 12 items of the display exactly one time.

2.2. *Experiment setup, off- and online protocols*

EEG signals were recorded with a g.HIamp and a g.EEGcap (Guger Technologies, Graz, Austria) with a sensitivity of $100\,\mu$V, band pass filtered between 0.1 and 60 Hz, and sampled at 512 Hz. We recorded from EEG electrode positions Fz, Cz, Pz, Oz, F3, F4, C3, C4, P7, P3, P4, P8, O1 and O2 from the extended International 10-20 system.[22,46,50,53] The right mastoid electrode was used as the reference, and the front electrode (FPz) was used as a ground.

During offline calibration, there were 16 trials per trial-block (i.e. 12 flashes per trial*16 trials = 168 flashes per trial-block); thus, each target item flashed 16 times during each trial-block. Each run consisted of five trial-blocks, each of which involved a different

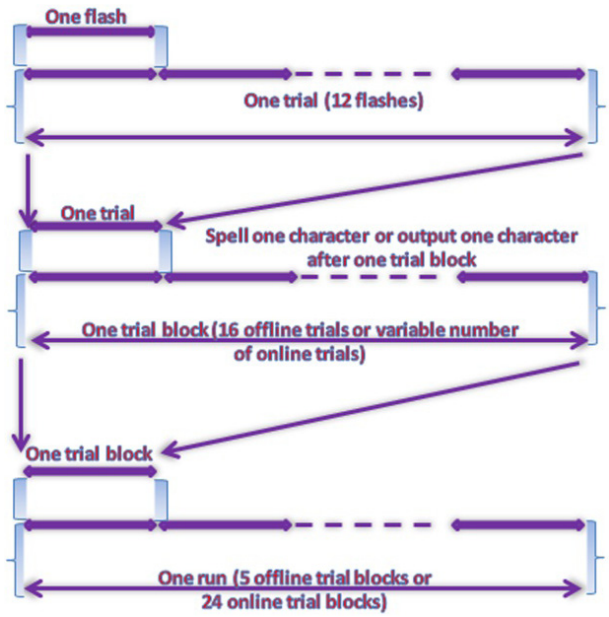

Fig. 2. One run of the experiment for online and offline experiments.

target character. During online testing, the number of trials per trial-block was variable, because the system optimized performance, as described in Sec. 2.5. Copy spelling was used in the off- and online phases of the study; a cue (green rectangle; Fig. 1(b)) was shown for 2 s before each trial-block to orient the subject to the current target item.

Subjects completed three offline runs for the SC-pattern and three runs for the MSC-pattern (each run contained five trial-blocks). The order of the two paradigms was counterbalanced across subjects. After each paradigm, subjects were given a five-min break. Following the offline experiment, for each paradigm, there was one online run that consisted of 24 trial-blocks (see Fig. 2). The paradigms were presented in the same order as the offline runs. Between each online experiment, subjects were given a two-min break. Each subject completed all of the conditions in one experimental session.

2.3. *Feature extraction procedure*

A third-order Butterworth band pass filter was used to filter the EEG between 0.1 and 30 Hz.[54,55] The first 800 ms of EEG after presentation of a single stimulus was used to extract the feature from each channel. A pre-stimulus interval of 100 ms was used for baseline correction of single trials in ERP analysis. Raw feature of each channel was downsampled from 512 to 73 Hz by selecting every seventh sample from the filtered EEG. The raw feature matrix is 14×406 for each single flash. Here, "14" is the number of the channels. The size of the feature vector is 14×58 (14 channels by 58 time points).

2.4. *Classification scheme*

Bayesian linear discriminant analysis (BLDA) is an extension of Fisher's linear discriminant analysis (FLDA). Data acquired offline were used to train the classifier using BLDA and obtain the classifier model. This model was then used in the online system. The item receiving the highest classifier output value was identified as the target character. BLDA uses regularization to prevent overfitting to high dimensional and possibly noisy datasets. Using a Bayesian analysis, the degree of regularization can be estimated automatically and quickly from training data without the need for time consuming cross-validation.[22] Assume that the target t and feature vectors $\mathbf{x}$ are linearly related with additive white Gaussian noise n:

$$t = \mathbf{w}^T\mathbf{x} + n. \tag{1}$$

Equation (3) is the likelihood function for the weight $\mathbf{w}$ used in regression:

$$p(\mathbf{D} \mid \beta, \mathbf{w}) = \left(\frac{\beta}{2\pi}\right)^{\frac{N}{2}} \exp\left(-\frac{\beta}{2}\|\mathbf{X}^T\mathbf{w} - \mathbf{t}\|^2\right). \tag{2}$$

Here, $\mathbf{t}$ denotes a vector containing the regression targets, $\mathbf{X}$ denotes the matrix that is obtained from the horizontal stacking of the training feature vectors, $\mathbf{D}$ denotes the pair $\{\mathbf{X}, \mathbf{t}\}$, β denotes the inverse variance of the noise, and N denotes the number of examples in the training set.

In the Bayesian setting, a prior distribution was specified for the latent variables $\mathbf{w}$ as:

$$p(\mathbf{w} \mid \alpha) = \left(\frac{\alpha}{2\pi}\right)^{\frac{D}{2}} \left(\frac{\varepsilon}{2\pi}\right)^{\frac{1}{2}} \exp\left(-\frac{1}{2}\mathbf{w}^T\mathbf{I}'(\alpha)\mathbf{w}\right). \tag{3}$$

$\mathbf{I}'(\alpha)$ is a $(D+1)$-dimensional diagonal matrix (D is the size of the features).

$$\mathbf{I}'(\alpha) = \begin{bmatrix} \alpha & 0 & \cdots & 0 \\ 0 & \alpha & \cdots & 0 \\ \vdots & \vdots & \ddots & \vdots \\ 0 & 0 & \cdots & \varepsilon \end{bmatrix}. \tag{4}$$

The posterior distribution can be computed by using Bayes rule:

$$p(\mathbf{w} \mid \beta, \alpha, \mathbf{D}) = \frac{p(\mathbf{D} \mid \beta, \mathbf{w})p(\mathbf{w} \mid \alpha)}{\int p(\mathbf{D} \mid \beta, \mathbf{w})p(\mathbf{w} \mid \alpha)d\mathbf{w}}. \tag{5}$$

The predictive distribution is obtained by multiplying Eq. (3) for a new input vector and Eq. (6):

$$p(\hat{t} \mid \beta, \alpha, \hat{\mathbf{x}}, \mathbf{D}) = \int p(\hat{t} \mid \beta, \mathbf{w})p(\mathbf{w} \mid \beta, \alpha, \mathbf{D})d\mathbf{w}. \tag{6}$$

The predictive distribution can be characterized by its mean μ and its variance $\sigma^2\sigma^2$:

$$\mu = \mathbf{m}^T\hat{\mathbf{x}}, \tag{7}$$

$$\sigma^2 = \frac{1}{\beta} + \hat{\mathbf{x}}^T\mathbf{C}\hat{\mathbf{x}}. \tag{8}$$

All the details could be found in Ref. 22.

2.5. *Adaptive system settings*

The number of trials per average was automatically selected based on the classifier output. After each trial, the classifier would determine the target character based on data from all trials in the specific trial-block. If the classifier chose the same item after two successive trials, the trial-block was terminated and the selected item was presented to the subject as feedback. For example, if the classifier selected "A" after the first trial, a second trial was presented. The data from both trials was averaged, and if the classifier selected "A" a second time no additional trials would be presented. If the classifier did not select "A", another trial would begin, and so on until cha (n) = cha $(n-1)$ or until 16 trials were presented. After 16 trials, the classifier would automatically select the item with the highest classifier output.[28]

2.6. *Subjective report*

After completing the last run, each subject was asked two questions about each of the two conditions. These questions could be answered on a 1–5 scale indicating strong disagreement, moderate disagreement, neutrality, moderate agreement, or strong agreement. The two questions were:

(i) Were you attracted to the background at the target location?
(ii) Did you perceive a distinct change in the shape of the matrix each time a flash occurred?

The questions were asked in Mandarin Chinese.

3. Results

Figure 3 shows the grand averaged amplitude of target stimuli for all subjects and all 14 electrode locations used for classification. Figure 3 clearly shows notable differences between the SC- and MSC-patterns. Averaged across all subjects, amplitude and latency values for the components of interest (i.e. N200, P300 and N400) are shown in Table 1.

Mean amplitude of the averaged ERPs (±25 ms) were compared between the two patterns using paired samples t-tests (see Fig. 4). Electrode locations P8 and Oz were selected for the N200 analysis because MMN is typically largest in occipital areas.[47,49,50,56] Electrode location Pz was selected for the P300 analysis because is commonly largest at Pz.[17] Electrode location Cz was selected for the N400 analysis because it typically contains the largest N400.[57]

Given that the N200 was compared at two electrode locations, a Bonferoni–Holm correction was used ($\alpha = 0.025$). At electrode P8, although 7 of 10 subjects showed larger N200s for the MSC-pattern, a statistically significant difference was not observed ($t = 2.2$, $p > 0.025$, Fig. 4(a)). At electrode Oz, N200 amplitude of the MSC-pattern was significantly higher than the SC-pattern ($t = 3.7$, $p < 0.025$, Fig. 4(b)). At electrode Pz, the differences in P300 amplitude for the two conditions did not reach statistical significance ($t = 1.6$, $p = 0.1$, Fig. 4(c)). At electrode Cz, the amplitude of the N400 for the MSC-pattern was significantly higher than the SC pattern ($t = 2.5$, $p < 0.05$, Fig. 4(d)).

Figure 5 shows the topographic map and time energy figure of r-squared values during presentation of the MSC-pattern and the SC-pattern. It can be seen that the MSC-pattern produced higher r-squared values than the SC-pattern for each of the three components. The average P300 r-squared values were significantly higher for the MSC-pattern than for the SC-pattern ($t = 3.8$, $p < 0.05$). As a discriminant index, the pointwise biserial correlation coefficient is defined as

$$r(x) = \frac{\sqrt{N_1 N_2}}{N_1 + N_2} \cdot \frac{\text{mean}\{x_i \,|\, l_i = 1\} - \text{mean}\{x_i \,|\, l_i = 2\}}{\text{std}\{x_i \,|\, l_i = 1, 2\}}, \quad (9)$$

where N_1 and N_2 are the number of variables belong to the class 1 and class 2, respectively, x_i and l_i are the value and class label of the ith variable and r-squared value is equal to the square of $r(x)$.

Table 2 shows online classification accuracy, bit rate and number of trials for each paradigm. Paired samples t-tests were used to examine differences between the MSC- and SC-patterns. Classification accuracy and bit rate for the MSC-pattern were significantly higher than the SC-pattern ($t = 3.14$, $p < 0.05$; and $t = 3.79$, $p < 0.05$, respectively). The difference in the number of trials presented was not statistically significant ($t = 1.3$, $p > 0.05$).

Table 3 shows subjects' responses to the two questions. A paired-samples t-test was used to examine mean differences between the MSC- and

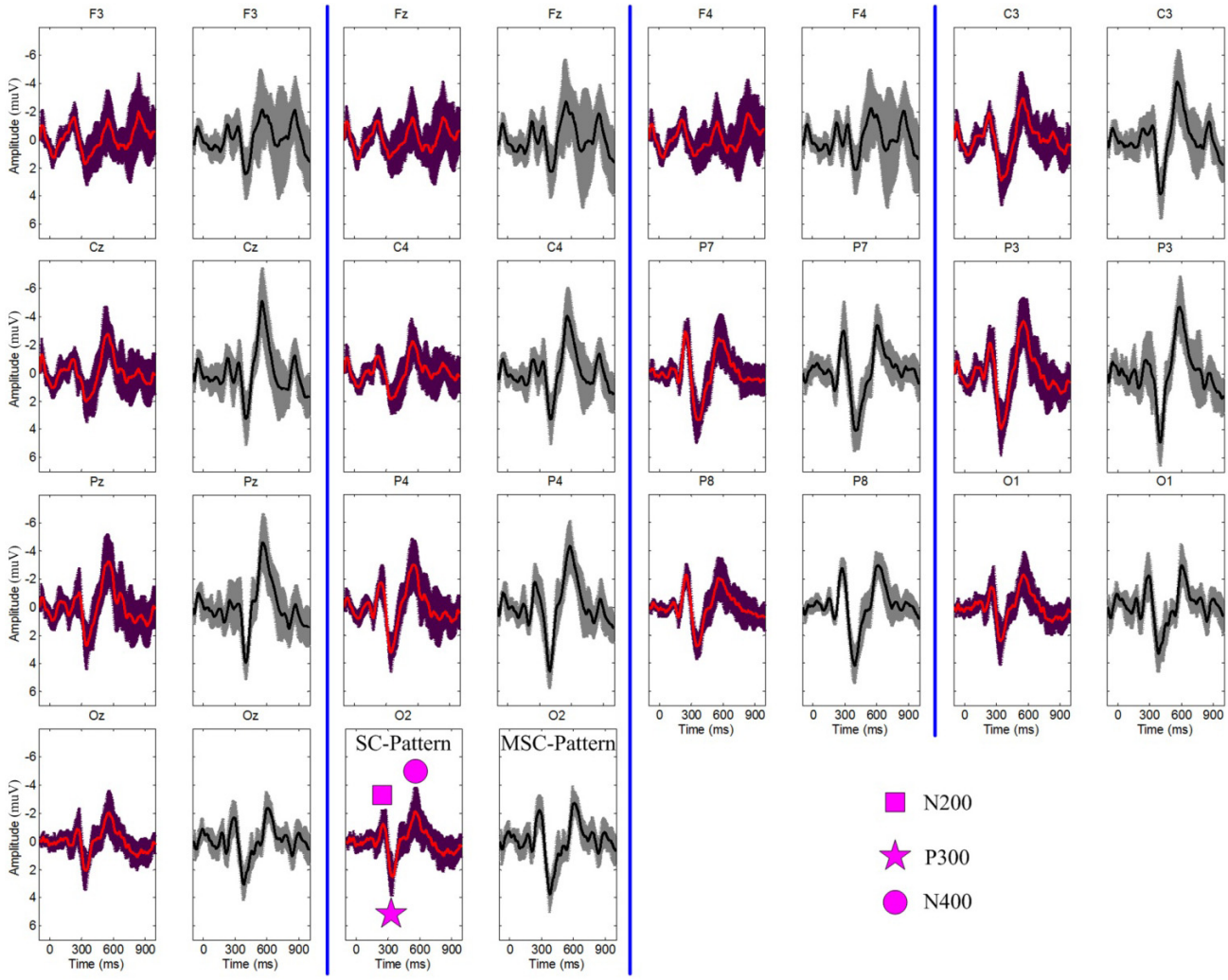

Fig. 3. Grand averaged ERPs of target stimuli across subjects 1-10 over 14 sites. Zero point is the beginning point of the target flash. The fringe of the shadow in each figure is the standard deviation of the ERP amplitude.

Table 1. Averaged peak values of N200 at P8 and Oz, P300 at Pz and N400 at Cz. "SC-P" denotes the single character pattern and "MSC-P" denotes the mismatch single character.

		Amplitude (μV)		Latency (ms)	
ERP	Electrodes	SC-P	MSC-P	SC-P	MSC-P
N200	P8	-2.52 ± 0.47	-3.12 ± 0.64	262 ± 19	278 ± 21
N200	Oz	-1.64 ± 0.83	-2.38 ± 1.01	241 ± 51	245 ± 78
P300	Pz	3.37 ± 1.36	4.18 ± 1.01	372 ± 37	397 ± 12
N400	Cz	-3.62 ± 1.30	-5.15 ± 2.38	576 ± 63	571 ± 48

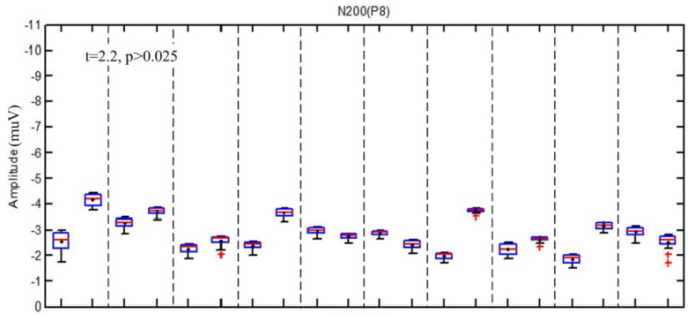

(a)

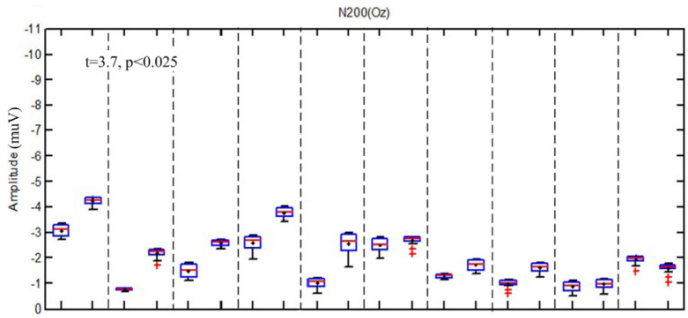

(b)

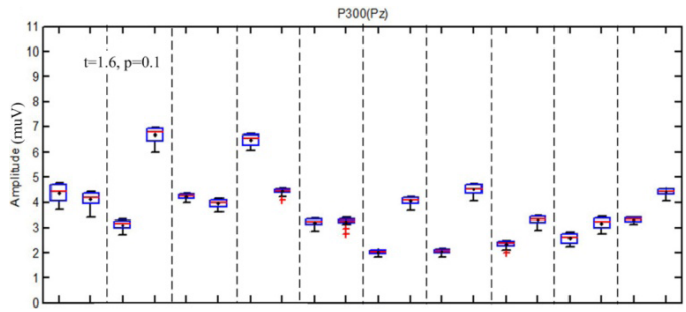

(c)

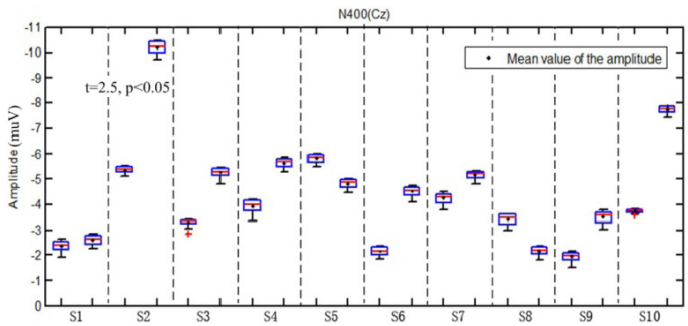

(d)

Fig. 4. Amplitude box plots for each subject at four electrode locations (P8, Oz, Pz and Cz). Amplitude is averaged from the maximum peak value ±25 ms for each electrode location. For each subject, the plot on the left represents the value for the SC-Pattern, and the plot on the right represents values for the MSC-pattern.

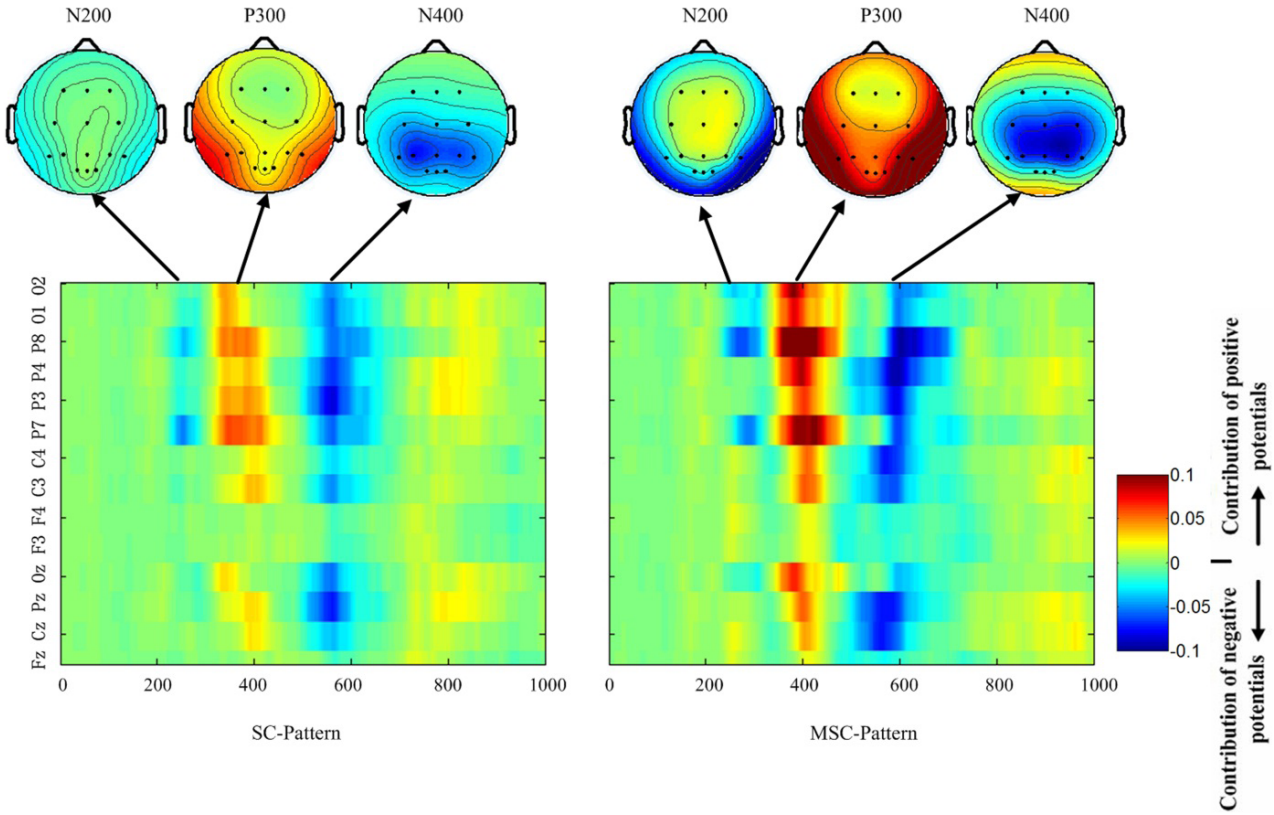

Fig. 5. Comparison of the topographic maps and time energy of r-squared values for SC-P and MSC-P; y-coordinate is channel and x-coordinate is time (ms).

Table 2. Online classification accuracy, bit rate and average number of trials for each subject. Acc = classification accuracy, RBR = raw bit rate (bits/min), AVT = average number of trials used to classify each character, SC-P = single character pattern, MSC-P = mismatch single character pattern, Avg is average and STD is standard deviation.

		S1	S2	S3	S4	S5	S6	S7	S8	S9	S10	Avg ± STD
Acc (%)	SC-P	95.8	91.7	100	100	95.8	70.8	91.7	100	83.3	83.3	91.3 ± 9.5
	MSC-P	95.8	100	100	100	100	83.3	100	100	100	95.8	97.5 ± 5.3
RBR (bit/s)	SC-P	24.5	21.4	26.1	26.6	24.5	11.2	18.9	24.7	17.2	16.0	21.1 ± 5.1
	MSC-P	24.1	23.5	26.6	28.7	28.7	17.2	27.5	26.1	24.3	24.5	25.1 ± 3.4
AVT	SC-P	2.17	2.25	2.29	2.25	2.17	2.54	2.54	2.42	2.29	2.46	2.34 ± 0.14
	MSC-P	2.21	2.54	2.25	2.08	2.08	2.29	2.17	2.29	2.46	2.17	2.25 ± 0.15

Table 3. Subjects' responses to two questions for each of the two patterns. IMP = question 1, SHC- = question 2, SC-P = single character pattern, MSC-P = mismatch single character pattern, Avg = average and STD = standard deviation.

		S1	S2	S3	S4	S5	S6	S7	S8	S9	S10	Avg ± STD
IMP	SC-P	2	3	3	2	3	2	2	2	3	3	2.5 ± 0.5
	MSC-P	4	4	5	5	5	4	5	4	4	4	4.4 ± 0.5
SHC	SC-P	2	3	3	3	3	3	2	3	1	3	2.6 ± 0.7
	MSC-P	4	4	5	4	5	4	4	4	4	5	4.3 ± 0.5

SC-patterns. Subjects reported having a stronger perception of the target stimulus in the MSC-pattern condition than in the SC-pattern condition ($t = 8.1$, $p < 0.05$). Table 3 also shows that the subjects reported a stronger perception of shape change in the MSC-pattern condition than in the SC-pattern condition ($t = 8.0$, $p < 0.05$). In fact, all of the subjects reported that the background of the SC-pattern did not produce a perceived change in shape.

4. Discussion

In this study, we incorporated a vMMN presentation method into the P300 BCI. The visual MSC-pattern presented a "D" (deviant) above one item in the matrix and an "S" (standard) above all of the other items. The performance and ERP components of the MSC-pattern were compared to the performance and ERP components of a SC-pattern. The SC-pattern was identical to the MSC-pattern except that the Ss were not presented. Thus, the SC-pattern is equivalent to the presentation method used in Ref. 52. As hypothesized, consistent with an MMN, N200 amplitude was significantly higher in the MSC-pattern than in the SC-pattern. In addition, classification accuracy and bit rate were significantly higher for the MSC-pattern. N400 amplitude was also statistically higher in the MSC-pattern. It is probable that the improved performance is due to the significant increases in N200 and N400 amplitude elicited by the MSC-pattern.

The resultant data produced several noteworthy findings. First, consistent with the MMN literature, the ERP data showed that a visual MMN was elicited when a stimulus was incongruent with the sensory memory trace of a standard stimulus.[48,58,59] Previous research has shown that the MMN will not be elicited without establishing a predictive model of the standard stimulus.[60] In this study, multiple presentations of the standard (S) stimulus at the target location established a predictive model of the standard stimulus, and the model was disrupted by presentations of the target (D) stimulus. The results showed that N200 amplitude for the MSC-pattern was significantly larger than the N200 for the SC-pattern, suggesting that a predictive model of the expected stimulus was established. Moreover, all of the subjects reported that the target stimulus was more salient for the MSC-pattern than for the SC-pattern,[61] this too provides additional support for the establishment of a predictive model of the standard (S) stimulus. Second, the two paradigms produced statistically similar P300s. This finding is expected because both paradigms should elicit a P300. The P300 reflects broad recognition and memory-updating processes that reflects identifying an attended to event and context updating processes[60,62–65]; the two paradigms are equivalent in terms attending to target stimuli and context updating. Third, the N400 is commonly elicited by unexpected words in sentences (e.g. see Ref. 65). In this experiment, we had no *a priori* reason to expect significantly larger N400s in the MSC-pattern. However, the results showed that the MSC-pattern elicited significantly larger N400s than the SC-pattern. A possible explanation for this finding is that the MSC-pattern produced a coherent pattern that provided a clear mismatch of shape, which did not exist in the SC-pattern. This explanation is consistent with the findings of Szűcs *et al.*[53]; they reported that an N400 was elicited by category and shape mismatches. Similar results were reported by Wang *et al.*[66] In their experiment, subjects were shown four different types of stimulus pairs: the stimuli could match on color and shape features (match), match on color and have a different shape (shape mismatch), match on shape and have a different color (color mismatch), or both the shape and color could be different (conjunction mismatches). The results showed that the color mismatch and shape mismatch conditions produced larger N400s. This finding can be generalized to the present experiment. A shape mismatch was present in the MSC-pattern condition but not in the SC-pattern condition. In addition to the presence of the shape mismatch, subjects reported a perception of shape change in the MSC-pattern, which presumably increased the amplitude of the N400.

5. Conclusion

The P300 BCI is a modified version of the classic oddball paradigm. In this paper, a modified version of the MMN paradigm was incorporated into the P300 BCI. In comparison to a standard P300 BCI task, the MMN modification performed significantly better in terms of accuracy and bit rate. The stimuli in this study were single characters,

whereas most P300 BCI paradigms simultaneously present several characters. The primary advantage of presenting groups of characters is an increase in the overall speed of the system. Therefore, we suggest that future research should be conducted to determine if these results can generalize to groups of characters. As P300 BCI technology is transitioned to people with severe motor disabilities, the MMN pattern may provide higher rates of communication than a standard P300 BCI.

Acknowledgments

This work was supported in part by the Grant National Natural Science Foundation of China, under Grant Nos. 61203127, 91420302 and 61305028. This work was also supported by the Fundamental Research Funds for the Central Universities (WG1414005, WH1314023).

References

1. J. J. Vidal, Toward direct brain-computer communication, *Annu. Rev. Biophys. Bioeng.* **2**(1) (1973) 157–180.
2. M. Cheng, X. Gao, S. Gao and D. Xu, Design and implementation of a brain-computer interface with high transfer rates, *IEEE Trans. Biomed. Eng.* **49**(10) (2002) 1181–1186.
3. G. Pfurtscheller and C. Neuper, Motor imagery and direct brain-computer communication, *Proc. IEEE* **89**(7) (2001) 1123–1134.
4. E. W. Sellers and E. Donchin, A P300-based brain-computer interface: Initial tests by ALS patients, *Clin. Neurophysiol.* **117**(3) (2006) 538–548.
5. J. Jin, B. Z. Allison, E. W. Sellers, C. Brunner, P. Horki, X. Wang and C. Neuper, Optimized stimulus presentation patterns for an event-related potential EEG-based brain computer interface, *Med. Biol. Eng. Comput.* **49**(2) (2011) 181–191.
6. Y. Zhang, Q. Zhao, J. Jin, X. Wang and A. Cichocki, A novel BCI based on ERP components sensitive to configural processing of human faces, *J. Neural. Eng.* **9**(2) (2012) 026018.
7. Y. Wang, R. Wang, X. Gao, B. Hong and S. Gao, A practical VEP-based brain-computer interface, *IEEE Trans. Neural. Syst. Reha. Eng.* **14**(2) (2006) 234–239.
8. A. Ortiz-Rosario and H. Adeli, Brain-computer interface technologies: From signal to action, *Rev. Neurosci.* **24**(5) (2013) 537–552.
9. G. R. Mueller-Putz, C. Pokorny, D. S. Klobassa and P. Horki, A single-switch brain-computer interface based on passive and imagined movements: Towards restoring communication in minimally conscious patients, *Int. J. Neural. Syst.* **23**(2) (2013) 1250037.
10. J. Li, H. Ji, L. Cao, D. Zang, R. Gu, B. Xia and Q. Wu, Evaluation and application of a hybrid brain computer interface for real wheelchair control with multi-degrees of freedom, *Int. J. Neural. Syst.* **24**(4) (2014) 1450014.
11. W. Y. Hsu, Application of competitive Hopfield neural network clustering to brain-computer interface systems, *Int. J. Neural. Syst.* **22**(1) (2012) 51–62.
12. M. A. Lopez-Gordo, F. Pelayo, A. Prieto and E. Fernandez, An auditory brain-computer interface with accuracy prediction, *Int. J. Neural. Syst.* **22**(3) (2012) 1250009.
13. N. V. Manyakov, N. Chumerin and M. M. Van Hulle, Multichannel decoding for phase-coded SSVEP brain-computer interface, *Int. J. Neural. Syst.* **22**(5) (2012) 1250022.
14. A. Ortiz-Rosario, I. Berrios-Torres, H. Adeli and J. A. Buford, Combined corticospinal and reticulospinal effects on upper limb muscles, *Neurosci. Lett.* **561** (2014) 30–34.
15. J. Li, J. Liang, Q. Zhao, K. Hong and L. Zhang, Design of wheelchair assistive system directly steered by human thoughts, *Int. J. Neural. Syst.* **23**(3) (2013) 1350013.
16. A. Burns, H. Adeli and J. A. Buford, Brain-Computer Interface after Nervous System Injury, *Neuroscientist* **20**(6) (2014) 639–651.
17. L. A. Farwell and E. Donchin, Talking off the top of your head: Toward a mental prosthesis utilizing event-related brain potentials, *Electroencephalogr. Clin. Neurophysiol.* **70**(6) (1988) 510–523.
18. J. R. Wolpaw, N. Birbaumer, D. J. McFarland, G. Pfurtscheller and T. M. Vaughan, Brain-computer interfaces for communication and control, *Clin. Neurophysiol.* **113**(6) (2002) 767–791.
19. W. S. Pritchard, *Psychophysiology of P300*, *Psychol. Bull.* **89**(3) (1981) 506–540.
20. R. Fazel-Rezai, B. Z. Allison, C. Guger, E. W. Sellers, S. C. Kleih and A. Kübler, P300 brain computer interface: Current challenges and emerging trends, *Front. Neuroeng.* **5** (2012) 14.
21. D. J. Krusienski, E. W. Sellers, D. J. McFarland, T. M. Vaughan and J. R. Wolpaw, Toward enhanced P300 speller performance, *J. Neurosci. Methods* **167**(1) (2008) 15–21.
22. U. Hoffmann, J. M. Vesin, T. Ebrahimi and K. Diserens, An efficient P300-based brain-computer interface for disabled subjects, *J. Neurosci. Methods* **167**(1) (2008) 115–125.
23. A. Onishi, A. H. Phan, K. Matsuoka and A. Cichocki, Tensor classification for P300-based brain computer interface, in *Proc. 2012 IEEE Int. Conf. Acoustics, Speech, and Signal Processing* (2012), pp. 581–584.
24. Y. Zhang, G. Zhou, J. Jin, Q. Zhao, X. Wang and A. Cichocki, Aggregation of sparse linear discriminant

analyses for event-related potential classification in brain-computer interface, *Int. J. Neural. Syst.* **24**(1) (2014) 1450003.
25. G. Rodríguez-Bermúdez, P. J. García-Laencina and J. Roca-Dorda, Efficient automatic selection and combination of EEG features in least squares classifiers for motor-imagery brain computer interfaces, *Int. J. Neural. Syst.* **23**(4) (2013) 1350015.
26. H. Adeli, Z. Zhou and N. Dadmehr, Analysis of EEG records in an epileptic patient using wavelet transform, *J. Neurosci. Methods* **12**(1) (2003) 69–87.
27. A. Lenhardt, M. Kaper and H. J. Ritter, An adaptive P300-based online brain-computer interface, *IEEE Trans. Neural. Syst. Rehab. Eng.* **16**(2) (2008) 121–130.
28. J. Jin, B. Z. Allison, E. W. Sellers, C. Brunner, P. Horki, X. Wang and C. Neuper, An adaptive P300-based control system, *J. Neural. Eng.* **8**(3) (2011) 036006.
29. S. Lu, C. Guan and H. Zhang, Unsupervised brain computer interface based on intersubject information and online adaptation, *IEEE Trans. Neural. Syst. Rehab. Eng.* **17**(2) (2009) 135–145.
30. J. Jin, E. W. Sellers, Y. Zhang, I. Daly, X. Wang and A. Cichocki, Whether generic model works for rapid ERP-based BCI calibration, *J. Neurosci. Meth.* **212**(1) (2013) 94–99.
31. Y. Zhang, G. Zhou, Q. Zhao, J. Jin, X. Wang and A. Cichocki, Spatial-temporal discriminant analysis for ERP-based brain-computer interface, *IEEE Trans. Neural. Syst. Rehab. Eng.* **21**(2) (2013) 233–243.
32. S. M. Martens, N. J. Hill, J. Farquhar and B. Schölkopf, Overlap and refractory effects in a brain-computer interface speller based on the visual P300 event-related potential, *J. Neural. Eng.* **6**(2) (2009) 026003.
33. G. Townsend, B. K. LaPallo, C. B. Boulay, D. J. Krusienski, G. E. Frye, C. K. Hauser, N. E. Schwartz, T. M. Vaughan, J. R. Wolpaw and E. W. Sellers, A novel P300-based brain-computer interface stimulus presentation paradigm: Moving beyond rows and columns, *Clin. Neurophysiol.* **121**(7) (2010) 1109–1120.
34. J. Jin, B. Z. Allison, Y. Zhang, X. Wang and A. Cichocki, An ERP-based BCI using an oddball paradigm with different faces and reduced errors in critical functions, *Int. J. Neural. Syst.* **24**(8) (2014) 1450027.
35. C. L. Gonsalvez and J. Polich, P300 amplitude is determined by target-to-target interval, *Psychophysiology* **39**(3) (2002) 388–396.
36. B. Z. Allison and J. A. Pineda, Effects of SOA and flash pattern manipulations on ERPs, performance, and preference: Implications for a BCI system, *Int. J. Psychophysiol.* **59**(2) (2006) 127–140.
37. E. W. Sellers, D. J. Krusienski, D. J. McFarland, T. M. Vaughan and J. R. Wolpaw, A P300 event-related potential brain-computer interface (BCI): The effects of matrix size and inter stimulus interval on performance, *Biol. Psychol.* **73**(3) (2006) 242–252.
38. J. Jin, E. W. Sellers and X. Wang, Targeting an efficient target-to-target interval for P300 speller brain-computer interfaces, *Med. Biol. Eng. Comput.* **50**(3) (2012) 289–296.
39. K. A. Colwell, D. B. Ryan, C. S. Throckmorton, E. W. Sellers and L. M. Collins, Channel selection methods for the P300 speller, *J. Neurosci. Methods* **232** (2014) 6–15.
40. B. Hong, F. Guo, T. Liu, X. Gao and S. Gao, N200-speller using motion-onset visual response, *Clin Neurophysiol* **120**(9) (2009) 1658–1666.
41. J. Jin, B. Z. Allison, X. Wang and C. Neuper, A combined brain-computer interface based on P300 potentials and motion-onset visual evoked potentials, *J. Neurosci. Methods* **205**(2) (2012) 265–276.
42. R. Näätänen, A. W. Gaillard and S. Mäntysalo, Early selective-attention effect on evoked potential reinterpreted, *Acta Psychol. (Amst)* **42**(4) (1978) 313–329.
43. J. N. Hill, T. N. La, K. Bierig, N. Birbaumer and B. Schölkopf, An auditory paradigm for brain-computer interfaces, NIPS (2004), Available at http://papers.nips.cc/paper/2551-an-auditory-paradigm-for-brain-computer-interfaces.pdf.
44. S. Kanoh, K. Miyamoto and T. Yoshinobu, A brain-computer interface (BCI) system based on auditory stream segregation, *Conf. Proc. IEEE Eng. Med. Biol. Soc.* (2008), pp. 642–645.
45. R. Cammann, Is there a mismatch negativity (MMN) in visual modality? *Behav. Brain Sci.* **13**(2) (1990) 234–235.
46. M. Kimura, J. Katayama and H. Murohashi, Attention switching function of memory-comparison-based change detection system in the visual modality, *Int. J. Psychophysiol.* **67**(2) (2008) 101–113.
47. M. Kimura, E. Schröger, I. Czigler and H. Ohira, Human visual system automatically encodes sequential regularities of discrete events, *J. Cogn. Neurosci.* **22**(6) (2010) 1124–1139.
48. M. Kimura, Visual mismatch negativity and unintentional temporal-context-based prediction in vision, *Int. J. Psychophysiol.* **83**(2) (2012) 144–155.
49. A. Czigler, J. Weisz and I. Winkler, ERPs and deviance detection: Visual mismatch negativity to repeated visual stimuli, *Neurosci. Lett.* **401**(1–2) (2006) 178–182.
50. I. Czigler, Visual mismatch negativity and categorization, *Brain Topogr.* **27**(4) (2014) 590–598.
51. F. Cong, A.-H. Phan, Q. Zhao, T. Huttunen-Scott, J. Kaartinen, T. Ristaniemi, H. Lyytinen and A. Cichocki, Benefits of multi-domain feature of mismatch negativity extracted by non-negative tensor factorization from EEG collected by low-density array, *Int. J. Neural. Syst.* **22**(6) (2012) 1–19.

52. C. Guger, S. Daban, E. W. Sellers, C. Holzner, G. Krausz, R. Carabalona, F. Gramatica and G. Edlinger, How many people are able to control a P300-based brain-computer interface (BCI)? *Neurosci. Lett.* **462**(1) (2009) 94–98.
53. D. Szűcs, F. Soltész, I. Czigler and V. Csépe, Electroencephalography effects to semantic and non-semantic mismatch in properties of visually presented single-characters: The N2b and the N400, *Neurosci. Lett.* **412**(1) (2007) 18–23.
54. J. Kremláček, M. Kuba, Z. Kubová and J. Langrová, Visual mismatch negativity elicited by magnocellular system activation, *Vis. Res.* **46** (2006) 485–490.
55. G. Stefanics, G. Csukly, S. Komlósi, P. Czobor and I. Czigler, Processing of unattended facial emotions: A visual mismatch negativity study, *Neuroimage* **59** (2012) 3042–3049.
56. J. R. Folstein and C. V. Petten, Influence of cognitive control and mismatch on the N2 component of the ERP: A review, *Psychophysiology* **45**(1) (2008) 152–170.
57. C. C. Duncan, R. J. Barry, J. F. Connolly, C. Fischer, P. T. Michie, R. Näätänen and C. Van Petten, Event-related potentials in clinical research: Guidelines for eliciting, recording, and quantifying mismatch negativity, P300, and N400, *Clin. Neurophysiol.* **120**(11) (2009) 1883–1908.
58. R. Näätänen, *Attention and Brain Function* (Psychology Press, 1992).
59. M. Kimura, A. Widmann and E. Schröger, Top-down attention affects sequential regularity representation in the human visual system, *Int. J. Psychophysiol.* **77**(1) (2010) 126–134.
60. N. K. Squires, K. C. Squires and S. A. Hillyard, Two varieties of long-latency positive waves evoked by unpredictable auditory stimuli in man, *Electroencephalogr. Clin. Neurophysiol.* **38**(4) (1975) 387–401.
61. M. Kimura, J. Katayama and H. Murohashi, Probability-independent and -dependent ERPs reflecting visual change detection, *Psychophysiology* **43**(2) (2006) 180–189.
62. R. T. Knight, D. Scabini, D. L. Woods and C. C. Clayworth, Contributions of temporal-parietal junction to the human auditory P3, *Brain Res.* **502**(1) (1989) 109–116.
63. S. H. Patel and P. N. Azzam, Characterization of N200 and P300: Selected studies of the event-related potential, *Int. J. Med. Sci.* **2**(4) (2005) 147–154.
64. J. Polich, Updating P300: An integrative theory of P3a and P3b, *Clin. Neurophysiol.* **118**(10) (2007) 2128–2148.
65. M. Kutas and S. A. Hillyard, Reading senseless sentences: Brain potentials reflect semantic incongruity, *Science* **207**(4427) (1980) 203–205.
66. Y. Wang, L. Cui, H. Wang, S. Tian and X. Zhang, The sequential processing of visual feature conjunction mismatches in the human brain, *Psychophysiology* **41**(1) (2004) 21–29.